

DOI: 10.1002/((please add manuscript number))

Article type: Communication

Optical Lithography Patterning of SiO₂ Layers for Interface Passivation of Thin Film Solar Cells

*Sourav Bose, José M. V. Cunha, Sunil Suresh, Jessica De Wild, Tomás S. Lopes, João R. S. Barbosa, Ricardo Silva, Jérôme Borme, Paulo A. Fernandes, Bart Vermang and Pedro M. P. Salomé**

Sourav Bose, José M. V. Cunha, Tomás S. Lopes, João R. S. Barbosa, Ricardo Silva, Jérôme Borme, Paulo A. Fernandes, Pedro M. P. Salomé

INL – International Iberian Nanotechnology Laboratory, Avenida Mestre José Veiga, 4715-330 Braga, Portugal

E-mail: Pedro.Salome@inl.int

Sourav Bose

Ångström Laboratory, Solid State Electronics, Ångström Solar Center, Uppsala University, SE-751 21 Uppsala, Sweden

José M. V. Cunha, Pedro M. P. Salomé

Departamento de Física, Universidade de Aveiro, Campus Universitário de Santiago, 3810-193 Aveiro, Portugal

Sunil Suresh, Jessica De Wild, Bart Vermang

University of Hasselt—Partner in Solliance, Diepenbeek 3590, Belgium

Sunil Suresh, Jessica De Wild, Bart Vermang

IMEC—Partner in Solliance, Leuven 3001, Belgium

Sunil Suresh, Jessica De Wild, Bart Vermang

IMOMECE—Partner in Solliance, Diepenbeek 3590, Belgium

Paulo A. Fernandes

CIETI, Departamento de Física, Instituto Superior de Engenharia do Porto, Instituto Politécnico do Porto, Porto 4200-072, Portugal

Paulo A. Fernandes

I3N, Universidade de Aveiro, Aveiro 3810-193, Portugal

Keywords: Thin film solar cells; Cu(In,Ga)Se₂ (CIGS); defects passivation; semiconductors; optoelectronics

Abstract: Ultrathin Cu(In,Ga)Se₂ solar cells are a promising way to reduce costs and to increase the electrical performance of thin film solar cells. In this work, we develop an optical

lithography process that can produce sub-micrometer contacts in a SiO₂ passivation layer at the CIGS rear contact. Furthermore, an optimization of the patterning dimensions reveals constraints over the features sizes. High passivation areas of the rear contact are needed to passivate the CIGS interface so that high performing solar cells can be obtained. However, these dimensions should not be achieved by using long distances between the contacts as they lead to poor electrical performance due to poor carrier extraction. This study expands the choice of passivation materials already known for ultrathin solar cells and its fabrication techniques.

Cu(In,Ga)Se₂ solar cells have reached impressive values of power conversion efficiency, close to 23 %, with the introduction of a post-deposition treatment based in the introduction of alkali-metals that lower front interface recombination.^[1-3] By showing that the CIGS interfaces can improve significantly, passivation strategies also for the rear electrode have gained interest. It has been shown that a nanostructured Al₂O₃ layer with point-contacts can lead to significant increase in the efficiency of ultrathin devices by reduction of rear interface recombination.^[4-10] It has been demonstrated that due to low CIGS carrier lifetime values, the point contacts need to be separated by distances on the order of magnitude of the diffusion length (500-2000 nm),^[4,8-14] meaning that for a passivation area higher than 95 %, contacts with dimensions of one order of magnitude lower (50-200 nm) are needed. Hence, in previous studies, where the passivation effect has been demonstrated, the nanopatterning was made using e-beam lithography by creating a square array of contact circles.^[6,9,10] Attempts to use optical lithography have been reported that include the use of etched lines, or trenches, in an Al₂O₃ layer with a width of 3 μm and pitches varying from 6 to 30 μm.^[15] In this work, we expand the study of using photolithography to create a patterned insulator layer with etched features with 700 nm and 1400 nm which allow to increase the total passivation area while keeping the distance between the contacts the same order of magnitude as the carrier's diffusion length. Furthermore, according to recent studies indicating that SiO₂ is a promising passivation material, we choose to work with that dielectric material.^[16-21]

In this work, we study rear passivation effects on ultrathin CIGS solar cells. This passivation is performed by applying a SiO₂ layer, in a trench configuration, on top of the rear-contact electrode (Mo).^[22]

Atomic force microscope (AFM) is used in tapping mode with a scan rate of 1 Hz. J-V measurements are performed under a simulated and calibrated AM1.5 spectra (Oriel Instruments - PVIV Test Solution). External quantum efficiency (EQE) is measured using a

QEX10, with a monochromatic light scanned through the wavelength interval of 300 nm to 1100 nm with a step of 10 nm. Solar cell cross section images were taken with a Fei-NovaNanoSEM 650 high-resolution scanning electron microscope (SEM), with an acceleration voltage of 3 and 5 kV.

The SiO₂ layers are deposited using a SPTS CVD tool, with a 25 nm thickness on top of the Mo layer at a temperature of 300 °C. Prior to the photolithography process, the samples are coated with photoresist AZ1505 with a thickness of 600 nm. The exposure is done using a Direct Write Laser Lithography (DWL 2000) with a 405 nm laser line using a focus setting of 50 and an intensity of 60 % of the total laser output. The used pattern had dimensions of 40000 x 40000 nm and the exposures took around 20 minutes. Afterwards, the sample is developed for 60 seconds, using the developer AZ400K:H₂O 1:4. Afterwards, a physical etching process is performed through the dielectric exposing Mo, allowing for contact of the rear electrode to the CIGS. For this purpose, a reactive ion etching (RIE) process on SPTS ICP is used which according to our experience, does not change the contact properties of the Mo with CIGS.^[23] The system is capable of etching deep sub-micron features with near vertical sidewalls (anisotropic) and provides good selectivity. Helium gas is used for aiding backside cooling of the substrate. Ar, BCl₃ and Cl₂ are introduced into the main chamber. 3000KW & 13.56MHz RF Power Supply is used on the source generator achieving a selectivity of 0.4:1 of Al₂O₃ to AZ1505. Finally, to remove the remaining resist, the samples are dipped in acetone and put to ultrasound for 20 minutes. After that, the procedure is repeated using deionized water for 5 minutes.

Figure 1 shows a summary of the trenches fabrication steps used in this work and a schematic of the layers and the structures fabricated for the implementation of the rear contact passivation.

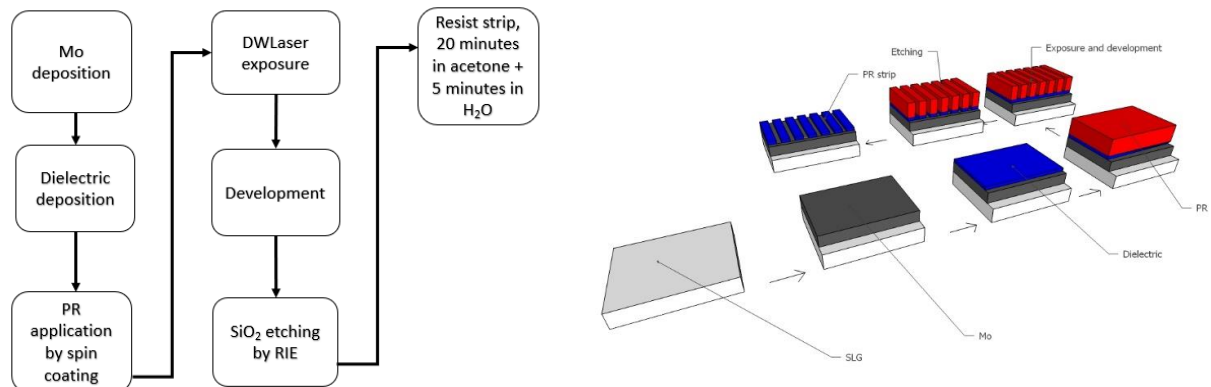


Figure 1 – Description of the fabrication process of the passivation layer.

Six sets of samples were fabricated. Each sample had a specific pattern and had 32 cells fabricated. The first set is a reference solar cell with the regular CIGS solar cell structure, SLG/Mo/CIGS/CdS/i-ZnO/ZnO:Al/Ni/Al/Ni grid. On all the other samples, SiO₂ was implemented as passivation layer, with the following structure: SLG/Mo/SiO₂/CIGS/CdS/i-ZnO/ZnO:Al/Ni/Al/Ni grid. The solar cell processing is explained in detail elsewhere ^[24] and for the CIGS, the layer was co-evaporated at 550 °C resulting in a thickness of 450 nm and composition $[Cu]/([Ga]+[In])=0.7$, $[Ga]/([Ga]+[In])=0.3$ as measured by X-ray fluorescence. Na was introduced as a NaF precursor layer with 3 nm. For the passivation sets, a trench configuration was implemented with line widths of 700 nm and 1400 nm, with variable pitch distances of 2, 4 and 8 μm. The pitch is defined as the inter-distance between the start of two consecutive lines, as shown in **Figure 2**.

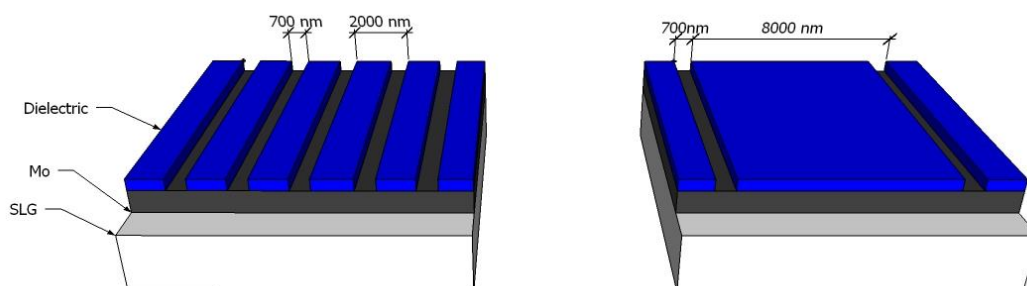


Figure 2 - Schematic showing some of the structures used: on the left sample H0.7Pitch2 and on the right sample H0.7Pitch8.

Summarized information is found in **Table 1** where the values of the contact and passivation area are also shown. With regards to the reference sample, we note that the substrates that

were used as references were from the same Mo batch and that these substrates were moved between processing together with the patterned substrates to ensure a fair comparison.^[25]

Table 1 - Summary of the samples produced in this work as well the exposure details. The sample naming follows the convention “Hx.x” for hole dimension, “Pitch” for the distance between holes with dimensions given in micrometers.

Sample name	Exposure details		
	Line Width (μm)	Pitch (μm)	Contact area (%)
H0.7Pitch2	0.7	2	35
H0.7Pitch4	0.7	4	17.5
H1.4Pitch4	1.4	4	35
H0.7Pitch8	0.7	8	8.75
H1.4Pitch8	1.4	8	17.5
Reference	No passivation layer		

As sub-micrometer features can be challenging to be fabricated using standard photolithography processes, a study of the substrate preparation is needed. Hence, AFM was used to investigate if the desired pattern is produced, as shown in **Figure 3** a) and b). All of the substrates showed precise well-defined trenches, however, here we only report on the results of a single pattern for simplicity reasons. The analysis shows a trench that is quite vertical with dimensions similar to the desired ones as expected since the RIE etching process we use provides quite vertical structures and has been optimized for these substrates. The line scan clearly shows that the SiO_2 layer was fully etched, i.e. Mo is exposed, as the hole has a depth of ~ 37 nm and the SiO_2 etched layer has a thickness of 25 nm, as showed in **Figure 3** c). The thickness difference is due to over-etching of the Mo, which we performed to ensure that the SiO_2 layer is uniformly open through the whole sample. A sub-micrometer opening of the SiO_2 layer is achieved, hence, the desired objective of having sub-micrometer openings performed by photolithography was accomplished.

Next, we performed SEM cross-section images of the complete solar cells to analyze if the SiO_2 layer located at the rear would significantly influence the morphology of the CIGS layer and to evaluate film adhesion. This analysis is also important to verify if the passivation layer survives the harsh CIGS growth conditions.

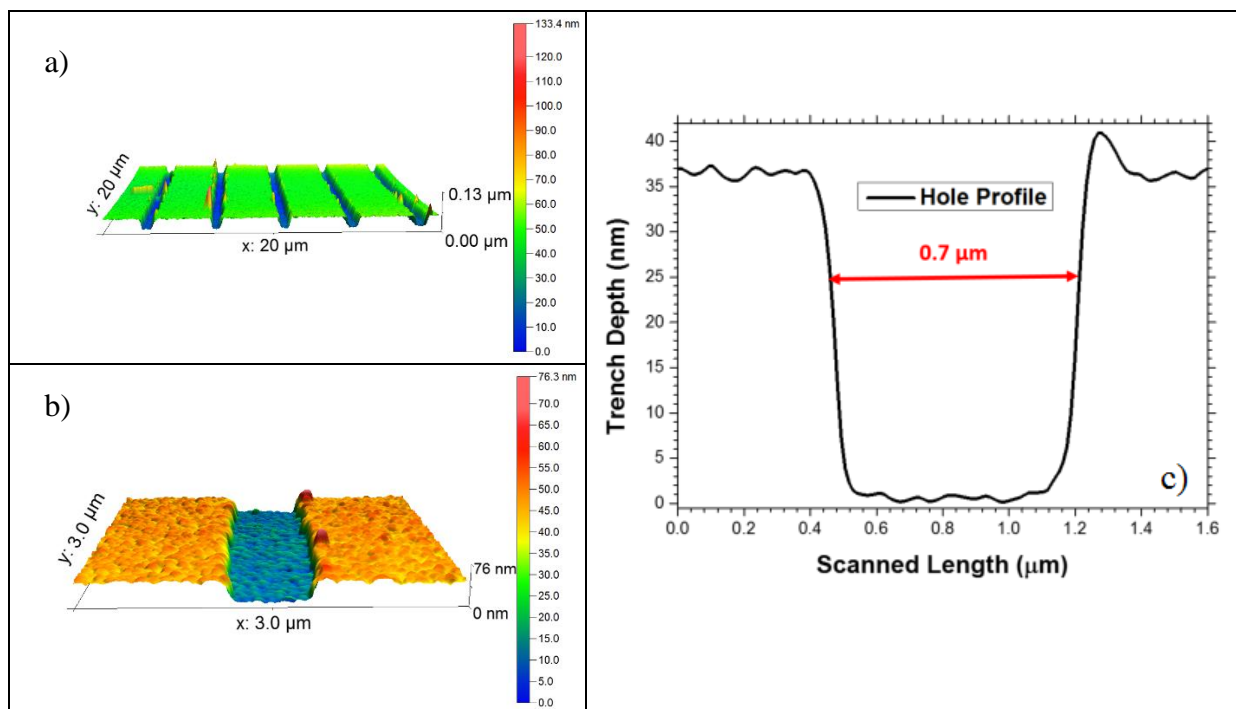


Figure 3 - AFM analysis of SLG/Mo/SiO₂ substrate. Both a) and b) show a 3D representation of sample H0.7Pitch2 and c) a depth line scan.

The reference solar cell and two samples, H0.7Pitch2 and H0.7Pitch8 were analyzed and the resulting images are shown in **Figure 4**. The SiO₂ layer, with 25 nm, is challenging to observe due to its thin thickness and its insulating properties, however, in **Figure 4** b) and c), dark layer is observed in between the Mo and the CIGS layer. In fact, in the case of the **Figure 4** c), a hole is present at the left part of the image (highlighted by a circle). These images show that the SiO₂ layer survives the harsh CIGS growth conditions and that there are no adhesion problems. Furthermore, all the samples show the same CIGS morphology with similar grain size, indicating that the SiO₂ layer did not make significant changes to the CIGS structure.

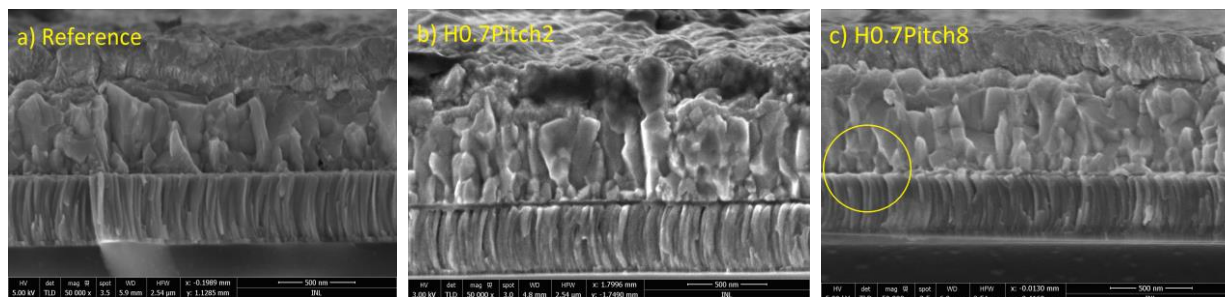


Figure 4 - SEM cross-section images of the following complete solar cells: a) reference, b) H0.7Pitch2 and c) H0.7Pitch8. The circular area of c) represents an opening in the SiO₂ layer.

Having shown that sub-micrometer features could be prepared with the desired specifications and that these substrates survive the CIGS growth process, we measured the J-V and EQE behavior of the resulting cells. Representative curves are shown in **Figure 5** and average and standard deviations values of the solar cell figures of merit are shown in **Table 2**. We note that the presented J_{sc} values are corrected with the EQE behavior using the AM1.5 spectra to obtain correct J_{sc} values which is a procedure usually needed in ultrathin devices. Hence, a small mismatch between the J-V representative curves and the EQE representative curves might exist. First, we note that this CIGS run has average quality as the reference device only achieves a power conversion efficiency value of 5 % and this cell suffers from shunting and series resistance as seen in the J-V plot. The reasons for this poor performance might be due to the low GGI composition, the use of a non-optimized alkali concentration, etc. If we only evaluate efficiency, then we notice that there are three passivation patterns that provide cells with an increase in efficiency of almost 1 % (abs.) compared with the reference devices. What is common to these three patterns is that its pitch distance is 2 and 4 μm . We note that sample H0.7Pitch4 has a slightly high V_{oc} and low J_{sc} value, which might be due to a small difference in the composition (GGI) and thickness values, however, the values are still close enough to be comparable. Nonetheless, we can gather the samples in two groups, the first group is where the samples both have an efficiency and a value of $V_{oc} * FF$ higher than the reference one. These samples, H0.7Pitch2, H0.7Pitch4 and H1.4Pitch4, show the typical effects of rear passivation by showing a moderate improvement in V_{oc} , a small improvement in J_{sc} and

similar values of FF as the reference devices.^[6,8,17,19] Hence, the hypothesis that SiO₂ could be used as a passivation material in CIGS is confirmed. The second group of samples with H0.7Pitch8 and H1.4Pitch8, are the ones where the pattern has a pitch of 8 μm between the SiO₂ openings. These samples show significant problems in carrier extraction as seen by its low values of FF and $V_{oc} * FF$, which results in efficiency values lower than the ones of the reference device. Such low values are indications of a high contact resistance of the rear electrode. The high contact resistance can be explained by hole accumulation in the rear interface and large values of current density in the small contacts that can lead to Auger recombination with negative impact in the solar cell performance.^[26] With regards to the passivation effect, we can focus on samples with the same pitch, so that the contact resistance is comparable, H0.7Pitch4 (580 mV) versus H1.4Pitch4 (521 mV) and H0.7Pitch8 (518 mV) versus H1.4Pitch8 (400 mV). Here, for the patterns with the same pitch, it is demonstrated that the pattern with the smaller trench dimension (i.e. the pattern with the highest passivation area) always shows the highest values of V_{oc} , a good indication that the rear recombination still has an effect. These results show that there are two effects that influence the electrical behavior of these solar cells. The first effect is connected with the pitch distance and in this experiment it is the dominant effect. If the pitch is too large, it will lead to high values of contact resistance resulting in a degradation of the solar cell performance. The second effect is the rear recombination, for the same pitch distance, high values of passivated area provide cells with better performance. A method to estimate contact resistance between these layers, like transmission line measurement (TLM), would be needed to extract definitive conclusions on the contact properties.

Furthermore, all of the passivated solar cells show a higher optical reflection in the long wavelength regime of the EQE behavior and also an increased J_{sc} . From modelling results it is known that the passivation of the rear interface leads to some increases in V_{oc} and to moderate increases in J_{sc} .^[4,8,10] Henceforward, part of the J_{sc} increase can be explained from the

passivation effects of the SiO₂ layer. However, the increased reflection of the devices is from light that is not absorbed by the CIGS, is reflected at the Mo/SiO₂, and exits the solar cell. Hence, the introduction of the SiO₂ layer changes the rear reflection but compared with the reference some light still exits the solar cell. Light trapping is then needed to take advantage of the rear increased optical reflection, in good agreement with other studies.^[17,19–21,27–30] From these simple measurements, it is hard to find a quantification on the increase of the J_{sc} between the increase in the reflection and the passivation effect.

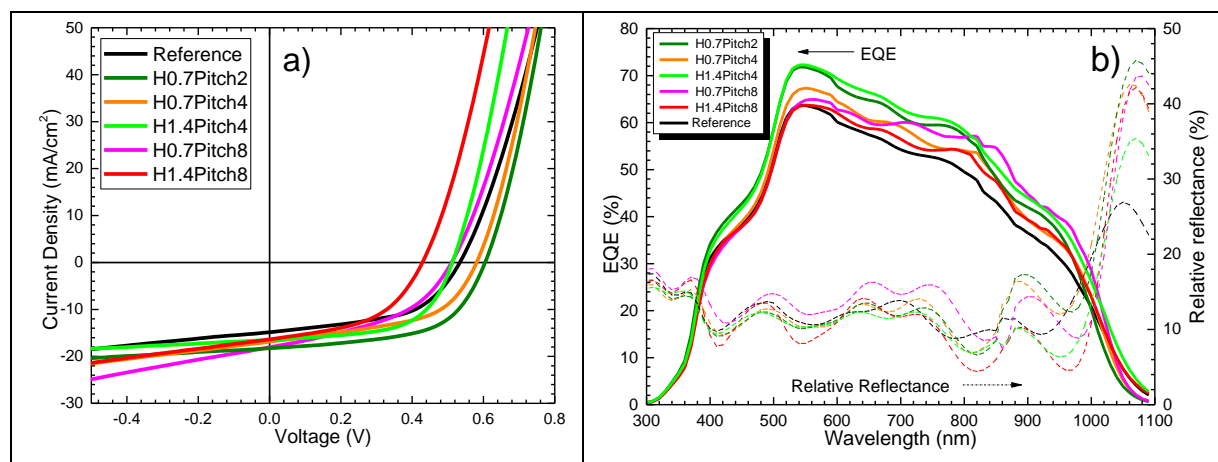


Figure 5 - a) J-V and b) EQE representative curves of a reference and of rear passivated solar cells. Figure b) also shows the reflectance relative to a BaSO₄ reference.

Table 2 - Average and standard deviations of 32 cells. The figure of merit Voc*FF, ideality factor, G_{shunt} and R_{series} are also presented.

	Graph colour code	J _{sc} ^{EQE} (mA/cm ²)	V _{oc} (mV)	FF (%)	Eff. (%)	V _{oc} * FF (mV)	Ideality Factor	G _{shunt} (mS.cm ⁻²)	R _{series} (Ohm.cm ⁻²)
H0.7Pitch2		18.22 ± 0.31	607 ± 5	52.2 ± 8.9	5.77 ± 0.99	315	2.4	1.88 ± 0.46	1.5±0.1
H0.7Pitch4		16.96 ± 0.39	580 ± 1	59.3 ± 4.2	5.84 ± 0.50	342	2.2	2.63 ± 1.67	1.4±0.2
H1.4Pitch4		18.73 ± 0.55	521 ± 30	59.1 ± 4.2	5.77 ± 0.58	307	2.0	2.20 ± 1.31	1.0±0.3
H0.7Pitch8		17.72 ± 1.09	518 ± 16	46.3 ± 6.1	4.28 ± 0.79	240	3.4	12.66 ± 13.04	2.6±0.7
H1.4Pitch8		16.81 ± 1.38	400 ± 23	42.0 ± 3.6	2.83 ± 0.44	168	3	7.34 ± 1.99	3.3±1.0
Reference		16.60 ± 0.94	536 ± 16	55.2 ± 3.4	4.93 ± 0.57	294	2.3	2.75 ± 0.58	1.7±0.5

In this paper we have shown that SiO₂ is a material that passivates the CIGS rear interface of ultrathin solar cells with gains in power conversion efficiency of 1 % (abs.) compared with reference devices. This study expands the choice of passivation materials already known^[22,31]

and its fabrication techniques. The most important conclusion from this paper is that for flat-Ga ultrathin CIGS solar cells, the pattern of the contacts on the passivation layer is quite important since two competing effects take place. On one hand, low values of contact area are needed to increase the effect of passivation, however, these values must not be made with large electrode distances as these increase contact resistance and lead to low FF and V_{oc} values. Hence, a passivation pattern that has very low contact areas that keeps its electrodes separated at sub-micrometer distances would be ideal.

We have shown that conventional lithography can be used for the creation of a passivation layer that leads to solar cells with power conversion efficiency values higher than reference devices, however, these patterns are likely not optimal and the use of this industrial-friendly technique needs to be optimized in future works. Furthermore, the SiO_2 layer itself can be optimized in terms of fixed electrical charge and thickness, important parameters for interface passivation.

Acknowledgements

Pedro M. P. Salomé acknowledges the funding of Fundação para a Ciência e a Tecnologia (FCT) through the project IF/00133/2015. José M. V. Cunha acknowledges the funding of Fundação para a Ciência e a Tecnologia (FCT) through the project PD/BD/142780/2018. Bart Vermang has received funding from the European Research Council (ERC) under the European Union's Horizon 2020 research and innovation programme (grant agreement no. 715027). The European Union's Horizon 2020 research and innovation programme ARCIIGS-M project (grant agreement no. 720887) is acknowledged. This research is also supported by Development of novel Ultrathin solar cell architectures for low-light, low-cost and flexible opto-electronic devices project (028075) co-funded by FCT and the ERDF through COMPETE2020.

Sourav Bose and José M. V. Cunha contributed equally to this work.

Received: ((will be filled in by the editorial staff))

Revised: ((will be filled in by the editorial staff))

Published online: ((will be filled in by the editorial staff))

References

- 1 E. Avancini, R. Carron, T. P. Weiss, C. Andres, M. Bürki, C. Schreiner, R. Figi, Y. E. Romanyuk, S. Buecheler and A. N. Tiwari, *Chem. Mater.*, 2017, **29**, 9695.

- 2 T. Feurer, P. Reinhard, E. Avancini, B. Bissig, J. Löckinger, P. Fuchs, R. Carron, T. P. Weiss, J. Perrenoud, S. Stutterheim, S. Buecheler and A. N. Tiwari, *Prog. Photovoltaics Res. Appl.*, 2017, **25**, 645.
- 3 P. Jackson, R. Wuerz, D. Hariskos, E. Lotter, W. Witte and M. Powalla, *Phys. status solidi – Rapid Res. Lett.*, 2016, **10**, 583.
- 4 B. Vermang, J. T. Watjen, C. Frisk, V. Fjallstrom, F. Rostvall, M. Edoff, P. Salome, J. Borme, N. Nicoara and S. Sadewasser, *IEEE J. Photovoltaics*, 2014, **4**, 1644.
- 5 B. Vermang, V. Fjällström, X. Gao and M. Edoff, *IEEE J. Photovoltaics*, 2014, **4**, 486–492.
- 6 P. M. P. Salomé, B. Vermang, R. Ribeiro-Andrade, J. P. Teixeira, J. M. V Cunha, M. J. Mendes, S. Haque, J. Borme, H. Águas, E. Fortunato, R. Martins, J. C. González, J. P. Leitão, P. A. Fernandes, M. Edoff and S. Sadewasser, *Adv. Mater. Interfaces*, 2018, **5**, 1701101.
- 7 D. Ledinek, P. Salome, C. Hagglund, U. Zimmermann and M. Edoff, *IEEE J. Photovoltaics*, 2018, **8**, 864.
- 8 B. Vermang, V. Fjällström, J. Pettersson, P. Salomé and M. Edoff, *Sol. Energy Mater. Sol. Cells*, 2013, **117**, 505–511.
- 9 B. Vermang, J. T. Wätjen, V. Fjällström, F. Rostvall, M. Edoff, R. Kotipalli, F. Henry and D. Flandre, *Prog. Photovoltaics Res. Appl.*, 2014, **22**, 1023.
- 10 S. Bose, J. M. V. Cunha, J. P. Teixeira, J. P. Leitão, J. Borme, J. Gaspar, P. A. Fernandes, M. Edoff and P. M. P. Salomé, *Submitt. to Thin Solid Film*.
- 11 J. Zhao, A. Wang and M. A. Green, in *IEEE Conference on Photovoltaic Specialists*, IEEE, 1990, pp. 333–335.
- 12 E. Schneiderlöchner, R. Preu, R. Lüdemann and S. W. Glunz, *Prog. Photovoltaics Res. Appl.*, 2002, **10**, 29.
- 13 T. Dullweber, S. Gatz, H. Hannebauer, T. Falcon, R. Hesse, J. Schmidt and R. Brendel,

- Prog. Photovoltaics Res. Appl.*, 2012, **20**, 630.
- 14 M. Moors, K. Baert, T. Caremans, F. Duerinckx, A. Cacciato and J. Szlufcik, *Sol. Energy Mater. Sol. Cells*, 2012, **106**, 84.
- 15 P. Casper, R. Hünig, G. Gomard, O. Kiowski, C. Reitz, U. Lemmer, M. Powalla and M. Hetterich, *Phys. Status Solidi - Rapid Res. Lett.*, 2016, **10**, 376–380.
- 16 J. M. V. Cunha, P. A. Fernandes, A. Hultqvist, J. P. Teixeira, S. Bose, B. Vermang, S. Garud, D. Buldu, J. Gaspar, M. Edoff, J. P. Leitao and P. M. P. Salome, *IEEE J. Photovoltaics*, 2018, 1.
- 17 C. van Lare, G. Yin, A. Polman and M. Schmid, *ACS Nano*, 2015, **9**, 9603.
- 18 G. Yin, M. Song, S. Duan, P. Manley, D. Greiner, C. A. Kaufmann and M. Schmid, *ACS Appl. Mater. Interfaces*, 2016, **8**, 31646.
- 19 G. Yin, P. Manley and M. Schmid, *Sol. Energy*, 2018, **163**, 443.
- 20 G. Yin, P. Manley and M. Schmid, *Sol. Energy Mater. Sol. Cells*, 2016, **153**, 124.
- 21 G. Yin, M. W. Knight, M.-C. van Lare, M. M. Solà Garcia, A. Polman and M. Schmid, *Adv. Opt. Mater.*, 2017, **5**, 1600637.
- 22 S. Garud, N. Gampa, T. G. Allen, R. Kotipalli, D. Flandre, M. Batuk, J. Hadermann, M. Meuris, J. Poortmans, A. Smets and B. Vermang, *Phys. Status Solidi A*, 2018, **215**, 1700826.
- 23 B. Vermang, Y. Ren, O. Donzel-Gargand, C. Frisk, J. Joel, P. Salome, J. Borme, S. Sadewasser, C. Platzer-Bjorkman and M. Edoff, *IEEE J. Photovoltaics*, 2016, **6**, 332–336.
- 24 S. Garud, B. Vermang, S. Sahayaraj, S. Ranjbar, G. Brammertz, M. Meuris, A. Smets and J. Poortmans, in *Physica Status Solidi (C) Current Topics in Solid State Physics*, 2017, vol. 14, pp. 2–7.
- 25 P. M. P. Salomé, V. Fjallstrom, A. Hultqvist, P. Szaniawski, U. Zimmermann and M. Edoff, *Prog. Photovoltaics Res. Appl.*, 2013, **22**, 83.

- 26 J. H. Werner, J. Mattheis and U. Rau, *Thin Solid Films*, 2005, **480–481**, 399.
- 27 M. Schmid, J. Klaer, R. Klenk, M. Topič and J. Krč, *Thin Solid Films*, 2013, **527**, 308.
- 28 G. Yin, V. Brackmann, V. Hoffmann and M. Schmid, *Sol. Energy Mater. Sol. Cells*, 2015, **132**, 142.
- 29 M. Schmid, *Semicond. Sci. Technol.*, 2017, **32**, 043003.
- 30 G. Yin, A. Steigert, P. Andrae, M. Goebelt, M. Latzel, P. Manley, I. Lauermann, S. Christiansen and M. Schmid, *Appl. Surf. Sci.*, 2015, **355**, 800.
- 31 A. S. Sokolov, S. K. Son, D. Lim, H. H. Han, Y.-R. Jeon, J. H. Lee and C. Choi, *J. Am. Ceram. Soc.*, 2017, **100**, 5638.

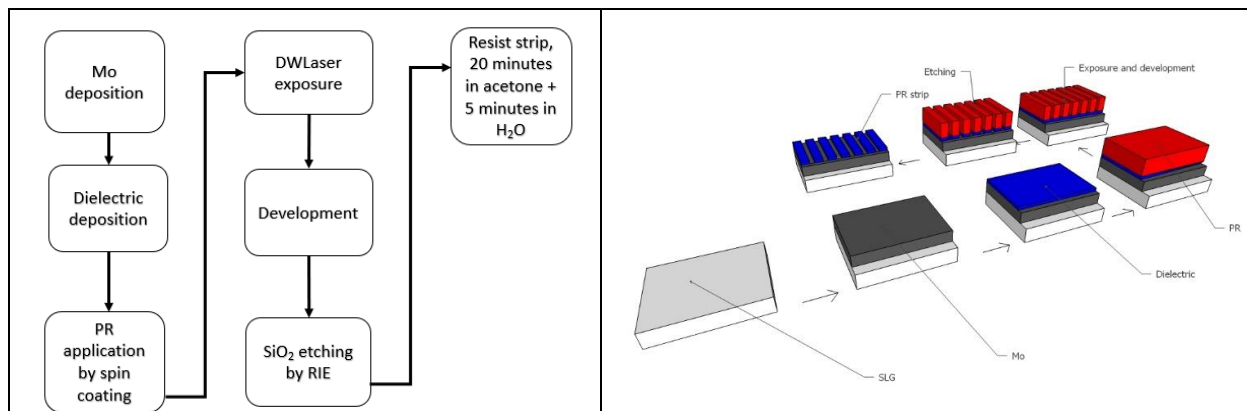


Figure 1 – Description of the fabrication process of the passivation layer.

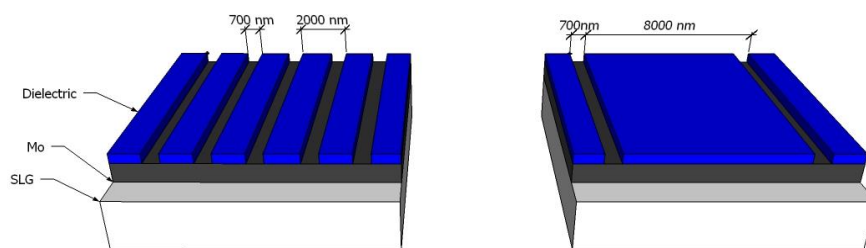


Figure 2 - Schematic showing some of the structures used: on the left sample H0.7Pitch2 and on the right sample H0.7Pitch8.

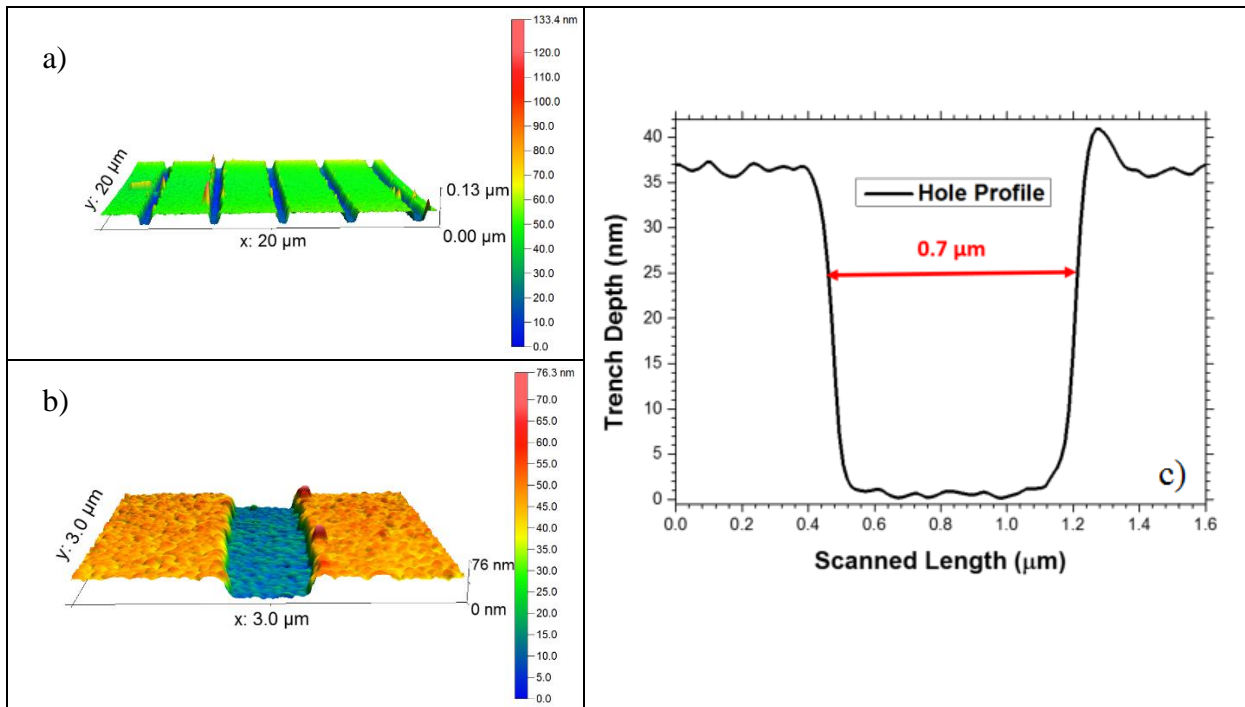


Figure 3 - AFM analysis of SLG/Mo/SiO₂ substrate. Both a) and b) show a 3D representation of sample H0.7Pitch2 and c) a depth line scan.

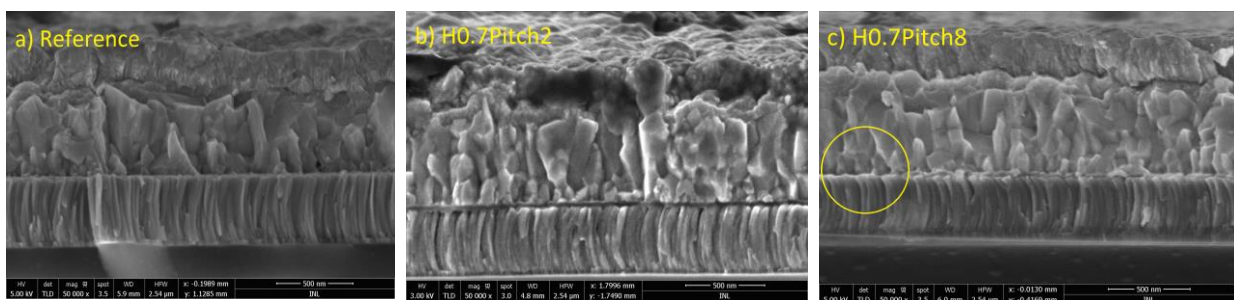


Figure 4 - SEM cross-section images of the following complete solar cells: a) reference, b) H0.7Pitch2 and c) H0.7Pitch8. The circular area of c) represents an opening in the SiO₂ layer.

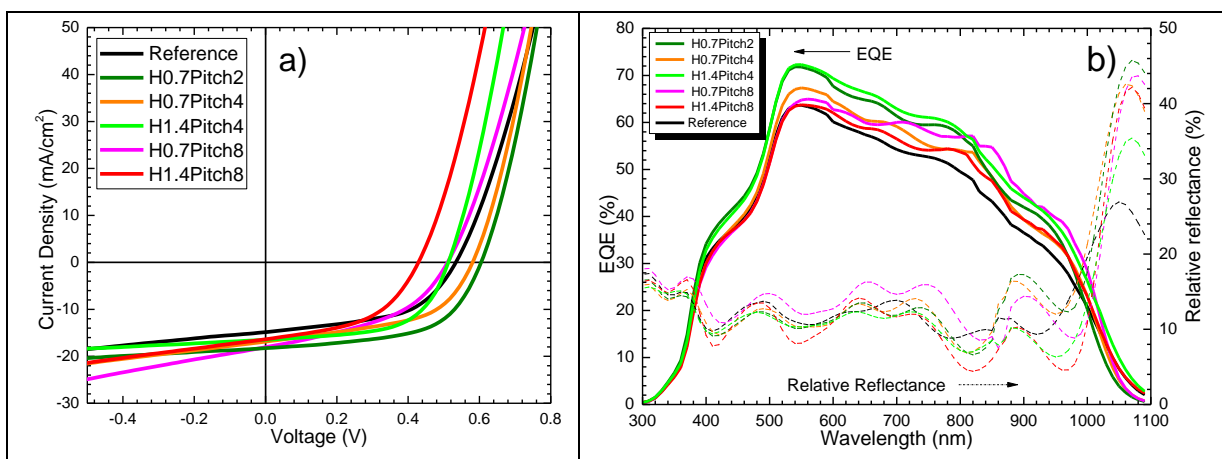








Figure 5 - a) J-V and b) EQE representative curves of a reference and of rear passivated solar cells.

Table 1 - Summary of the samples produced in this work as well the exposure details. The sample naming follows the convention “Hx.x” for hole dimension, “Pitch” for the distance between holes with dimensions given in micrometers.

Sample name	Exposure details		
	Line Width (μm)	Pitch (μm)	Contact area (%)
H0.7Pitch2	0.7	2	35
H0.7Pitch4	0.7	4	17.5
H1.4Pitch4	1.4	4	35
H0.7Pitch8	0.7	8	8.75
H1.4Pitch8	1.4	8	17.5
Reference	No passivation layer		

Table 2 - Average and standard deviations of 32 cells for each pattern.. The figure of merit Voc*FF, ideality factor, G_{shunt} and R_{series} are also presented.

	Graph colour code	J _{sc} ^{EQE} (mA/cm ²)	V _{oc} (mV)	FF (%)	Eff. (%)	V _{oc} * FF (mV)	Ideality Factor	G _{shunt} (mS.cm ⁻²)	R _{series} (Ohm.cm ²)
H0.7Pitch2		18.22 ± 0.31	607 ± 5	52.2 ± 8.9	5.77 ± 0.99	315	2.4	1.88 ± 0.46	1.5±0.1
H0.7Pitch4		16.96 ± 0.39	580 ± 1	59.3 ± 4.2	5.84 ± 0.50	342	2.2	2.63 ± 1.67	1.4±0.2
H1.4Pitch4		18.73 ± 0.55	521 ± 30	59.1 ± 4.2	5.77 ± 0.58	307	2.0	2.20 ± 1.31	1.0±0.3
H0.7Pitch8		17.72 ± 1.09	518 ± 16	46.3 ± 6.1	4.28 ± 0.79	240	3.4	12.66 ± 13.04	2.6±0.7
H1.4Pitch8		16.81 ± 1.38	400 ± 23	42.0 ± 3.6	2.83 ± 0.44	168	3	7.34 ± 1.99	3.3±1.0
Reference		16.60 ± 0.94	536 ± 16	55.2 ± 3.4	4.93 ± 0.57	294	2.3	2.75 ± 0.58	1.7±0.5

Keyword: Thin film solar cells; Cu(In,Ga)Se₂ (CIGS); defects passivation; semiconductors; optoelectronics

Sourav Bose, José M. V. Cunha, Sunil Suresh, Jessica De Wild, Tomás S. Lopes, João R. S. Barbosa, Ricardo Silva, Jérôme Borme, Paulo A. Fernandes, Bart Vermang and Pedro M. P. Salomé*

Optical Lithography Patterning of SiO₂ Layers for Interface Passivation of Thin Film Solar Cells

Figure 1 – Description of the fabrication process of the passivation layer. 5

Figure 2 - Schematic showing some of the structures used: on the left sample H0.7Pitch2 and on the right sample H0.7Pitch8. 5

Figure 3 - AFM analysis of SLG/Mo/SiO₂ substrate. Both a) and b) show a 3D representation of sample H0.7Pitch2 and c) a depth line scan. 7

Figure 4 - SEM cross-section images of the following complete solar cells: a) reference, b) H0.7Pitch2 and c) H0.7Pitch8. The circular area of c) represents an opening in the SiO₂ layer. 8

Figure 5 - a) J-V and b) EQE representative curves of a reference and of rear passivated solar cells..... 10

